Results in Chemistry 7 (2024) 101372

Contents lists available at ScienceDirect

Results in Chemistry

journal homepage: www.sciencedirect.com/journal/results-in-chemistry

Styryl carbamate backbones for the discovery of TME-disrupting agents

Amelia Bou-Puerto, Miguel Carda, Eva Falomir *

Departamento de Química Inorgánica y Orgánica, Universitat Jaume I, Castellón E-12071, Spain

ARTICLE INFO

Keywords:
Carbamate
Styryl unit
PD-L1
IL-6
TNF-α
SAA-1
THP-1
T cells
Monocyte
Tumor microenvironment
Antiproliferative activity
Anti-inflammatory effect

ABSTRACT

Twenty-one styryl carbamates have been designed, synthetized and characterized by their physical properties. Afterwards, their potential activity as tumor microenvironment disruptors has been evaluated. First, antiproliferative studies on tumor cell lines HT-29, A-549 and MCF-7 and on non-tumor cell line HEK-293 were carried out. Then, the antiproliferative activity of some selected compounds was evaluated on co-cultures of A-549 and immune cells, Jurkat T or monocytes THP-1. To determine their potential as oncoinflammation regulators, the secretion levels of IL-6, TNF-α and SAA-1 were, also, determined from these co-culture assays. Then, the effect on the expression levels of anticancer targets PD-L1 in both A-549 and monocytes THP-1 were established and, finally, the expression of CD80 and CD11b in THP-1. Compounds **9**–**13** bearing halophenyl carbamate units exhibited promising results as TME disruptors and inflammation regulators.

1. Introduction

Over the last decade there have been remarkable progress and improvement in cancer treatment approaches. One of the most outstanding advances in developing more effective therapies has been to consider not only the tumor cell as a target but also the entire ecosystem that surrounds it [1,2]. The first reason is that chemotherapies traditionally aimed at killing tumor cells are compromised by their own inaccessibility and secondly because tumor cells are not the only cells that might change their patterns of gene expression and metabolism during cancer progression [3]. Other cells that surround and interact with the tumor, such as endothelial or immune cells, play a vital role in determining how the tumor behaves. A full understanding of this tumor microenvironment (TME) includes the neoplastic cells and those cells that are recruited to help tumor cells survive and disseminate. It is this spread of cancer cells, or metastasis, that is the main cause of cancer-related mortality [4]. Unfortunately, once cancer cells have started their metastatic journey, standard medical interventions often only slow the progression of the disease. As a result, there remains a significant gap in the availability of therapies capable of disrupting this metastatic process [5,6,7]. It is therefore imperative to disrupt the intricate and intertwined networks that facilitate metastasis in TME. Although much remains to be discovered, regarding the intricate communication networks among diverse cell types within the tumor microenvironment (TME), emerging categories of therapies are focusing on these systems that sustain cancer [8,9]. Immune checkpoint inhibitors, antiangiogenic agents or compounds reducing the levels of some cytokines within TME exploit aspects of the TME to eliminate cancerous cells [10,11]. Notably, the inhibition of immune regulatory checkpoints, like the PD-1/PD-L1 axis, poses a significant challenge and opportunity in the realm of innovative oncology immunotherapies [12]. A prime illustration is pembrolizumab (Keytruda), an immune checkpoint inhibitor, which is an antibody used in clinical practice to hinder the activity of PD-L1, a protein that impedes the immune system. This interference enables immune cells to effectively target and eliminate cancer cells. PD-L1 can be present in cancer cells at levels exceeding 90 %, making it an exceptionally viable target. This class of immunotherapeutic drugs has been employed to treat various cancer types, occasionally inducing remission even in advanced cases. Nonetheless, its efficacy remains limited to only 20–30 % of patients [13]. However, these therapies may even fall short because they overlook the intricate tumor microenvironment (TME), where the secretion of pro-inflammatory and pro-angiogenic factors by tumor cells, coupled with the influx of inflammatory immune cells, fundamentally alters the TME's composition. This alteration obstructs anti-tumor immune responses [9] and fundamentally reshapes the behavior of immune cells like macrophages, better

* Corresponding author.
E-mail addresses: apuerto@uji.es (A. Bou-Puerto), mcarda@uji.es (M. Carda), efalomir@uji.es (E. Falomir).

https://doi.org/10.1016/j.rechem.2024.101372
Received 16 January 2024; Accepted 10 February 2024
Available online 15 February 2024

known as tumor-associated macrophages (TAMs) [14]. Within TAMs, pro-inflammatory cytokines, such as Interleukin-6 (IL-6) [9], which are excessively produced within the TME due to their release by tumor cells, assume a pivotal role in tumor growth and metastasis. Several investigations have indicated that IL-6 plays a role in the initiation and progression of tumors. IL-6 serves as a soluble mediator with diverse impacts on inflammation, the immune response and hematopoiesis [15,16]. Following its synthesis at a localized site during the initial stages of inflammation, IL-6 prompts the generation of a wide array of acute phase proteins [17], including SAA-1 [18]. It has been confirmed that there is a strong correlation between the levels of SAA-1 and IL-6 in the tumor microenvironment (TME) and the prognosis of cancer patients [17]. Furthermore, both SAA and IL-6 contribute to malignant progression in certain cancers such as gastric cancer (GCa) and non-small cell lung cancer (NSLC) [19,20,21].

Therefore, by targeting PD-L1 these therapies can help activate the immune system to recognize and attack cancer cells, potentially leading to more effective and durable anti-cancer responses.

In prior research, we developed scaffold structures for potential multitarget inhibitors through docking studies involving PD-L1 protein [22]. We based on crystal structure of BMS-202, a PD-L1 inhibitor, bound to the protein [23]. Compounds like BMS-202, created by Bristol-Myers Squibb, disrupt PD-1 and PD-L1 interaction by binding to a hydrophobic groove on PD-L1 comprising amino acids Tyr56, Met115, Ile116, Ala121 and Tyr123. This binding hampers PD-L1 dimerization, inhibiting the interaction through a two-fold process: obstructing the PD-1/PD-L1 connection and altering the PD-L1 dimer's conformation, preventing binding to PD-1. This results in the inactivation of PD-1 and PD-L1 interaction [24]. With this data and docking studies, we designed some scaffolds for the development of potential dual-targeting agents. Some of the designed molecules contained styryl urea units such as structures I and II in Fig. 1 [25,26]. These compounds reduced more than 80 % of the total PD-L1 compared to non-treated cancer cells. Besides, they exhibited immunomodulatory effects as they reduced the proportion of living cancer cells when co-cultured with T cells (Fig. 1).

More recently we have also been investigating the potential effect of these new molecules on TME [27,28]. Our aim in the present work was to make some structural modifications to our previously studied molecules such as styryl ureas I and II to study their effect on TME. Concretely, we aimed to study their effect on biological target PD-L1, their effect on the release of pro-inflammatory cytokines such as IL-6, TNF-α [29] and SAA-1 and their immunomodulatory effect. Our previous docking data on PD-L1 binding sites showed similar key data for urea and carbamate styryl units. Carbamate-bearing molecules play an important role in modern drug discovery and medicinal chemistry, mainly due to their chemical stability and capability to permeate cell membranes together with their unique ability to modulate inter- and intramolecular interactions with the target enzymes or receptors. We, therefore, decided to replace the urea with a carbamate group. We also decided to check the effect of the relative position of the amine group in the styryl unit by preparing a set of molecules with a *para*-amino group in the styryl group and another one with a *meta*-amino styryl unit (see Fig. 2). Fig. 3.

2. Results and discussion

2.1. Synthesis of styryl carbamate derivatives

The synthesis of the carbamate derivatives investigated in this study (see Scheme 1) was carried out in two steps. First, 1-methoxy-4-vinylbenzene was submitted to Heck reaction with 4-bromoaniline and 3-bromoaniline, in triethanolamine as solvent and in the presence of Pd $(AcO)_2$, as catalyst. After heating the reaction mixture at 100 °C for 72 h the intermediate (methoxystyryl)anilines **1** and **2** were achieved [30]. To obtain the carbamates, two procedures were applied. The vast majority of carbamates (see Fig. 1) were prepared by one-pot method (see conditions b in Scheme 1) in which the corresponding (methoxystyryl) aniline (**1** or **2**) was converted into trichloromethylcarbamates upon reaction with triphosgene and trimethylamine in THF. Then, trichloromethylcarbamates were transformed into carbamates by reaction with a range of phenols [31]. Carbamates **11**, **14**, **20** and **23** (see Fig. 1) were obtained upon reaction of the corresponding (methoxystyryl)aniline (**1** or **2**) with commercially available aryl chloroformates in THF in the presence of pyridine (see conditions c in Scheme 1). [32].

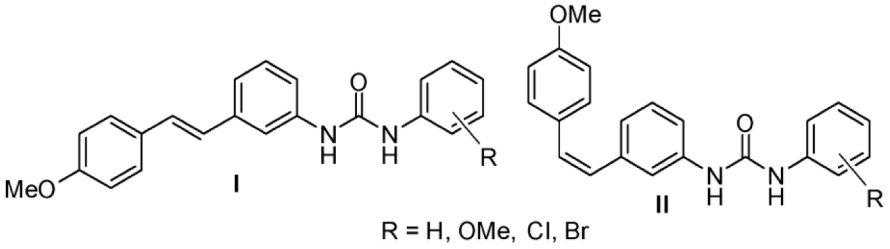

IC_{50} values for A-549 and HEK-293 and PD-L1 protein expression.

	A-549 (μM)	HEK-293 (μM)	t-PD-L1 (%)
Sorafenib	27 ± 2	5.0 ± 0.7	---
BMS-8	34 ± 2	16 ± 3	62 ± 3
(*E*)-*p*-Br	3.0 ± 0.4	0.7 ± 0.3	18 ± 5
(*Z*)-*p*-Br	12 ± 2	10 ± 2	17 ± 5

Fig. 1. Outstanding results from previously designed compounds compared to reference compounds.

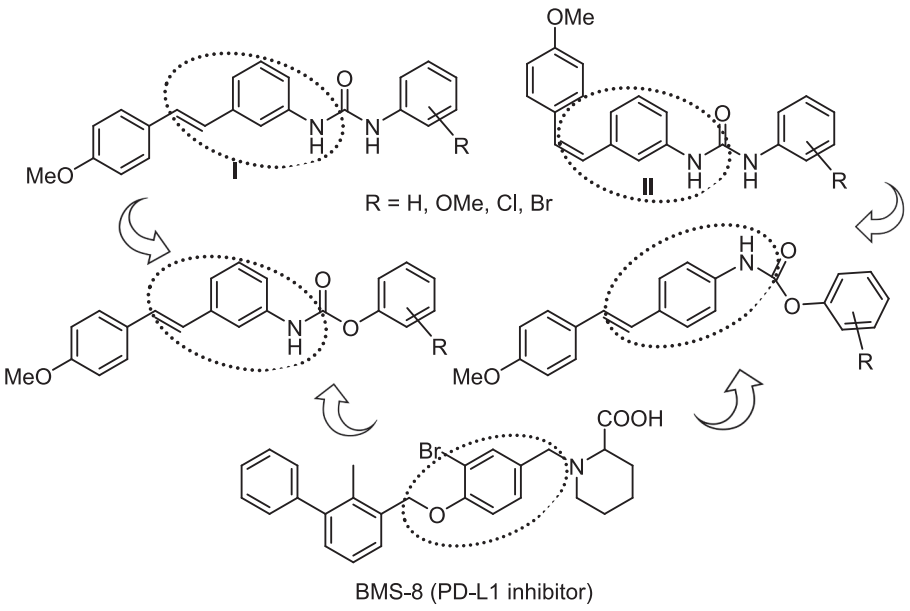

Fig. 2. New proposed structures as potential TME-disrupting agents.

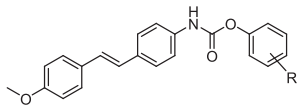

3. R = 2-CH_3 (method b, 37%)
4. R = 3-CH_3 (method b, 48%)
5. R = 4-CH_3 (method b, 45%)
6. R = 2-OCH_3 (method b, 37%)
7. R = 3-OCH_3 (method b, 41%)
8. R = 4-OCH_3 (method b, 39%)
9. R = 2-F (method b, 65%)
10. R = 3-F (method b, 47%)
11. R = 4-F (method c, 35%)
12. R = 2-Cl (method b, 64%)
13. R = 3-Cl (method b, 45%)
14. R = 4-Cl (method c, 36%)

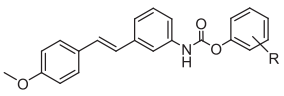

15. R = 2-CH_3 (method b, 43%)
16. R = 3-CH_3 (method b, 37%)
17. R = 4-CH_3 (method b, 40%)
18. R = 2-F (method b, 52%)
19. R = 3-F (method b, 54%)
20. R = 4-F (method c, 58%)
21. R = 2-Cl (method b, 47%)
22. R = 3-Cl (method b, 50%)
23. R = 4-Cl (method c, 60%)

Fig. 3. Structures of the carbamates investigated in this study.

2.2. Biological evaluation

2.2.1. Study of the effect on cell proliferation in monocultured cell lines

The ability of all the synthetized compounds to affect cell viability was studied by MTT assay using several human cell lines: HEK-293 (human embryonic kidney cells), HT-29 (colon adenocarcinoma), A-549 (pulmonary adenocarcinoma) and MCF-7 (breast adenocarcinoma).

We determined the corresponding IC_{50} values,expressed as μMconcentration, at which 50 % of cell viability, compared to non-treated one, is achieved. IC_{50} values are shown in Table 1 which also includes IC_{50} values for the reference compounds sorafenib and BMS-8.

In general, none of the compounds exhibited effect on HEK-293 at concentrations below 100 μM. Besides, compounds are more active against A-549 than in MCF-7 and HT-29. Moreover, it is observed that the *para*-aryl carbamate type derivatives are more active than the *meta*-aryl carbamate type and, furthermore, within each type, the haloaryl carbamate derivatives are the most active ones while the methylaryl carbamate are the less active of all the synthetized compounds. As regards the effect on A-549, we observed that most of the derivatives exhibited high nanomolar or low micromolar IC_{50} values, while in HT-29 only *para*-halophenyl carbamates are in the very low micromolar IC_{50} range. Finally, we observed that in MCF-7, again, *para*-halophenyl carbamates, together with *para*-*o*-methoxyphenyl **6** and *meta*-*p*-fluorophenyl carbamate **20,** exhibited high nanomolar IC_{50} values.

The morphology of the cells changed when treated with the compounds together with a reduction of the number of cells in the cultures. We observed that some cells had fibroblastic appearance (i) with shrinkage of the cytoplasm (ii) and chromatin condensation (iii) (see arrows in Fig. 4).

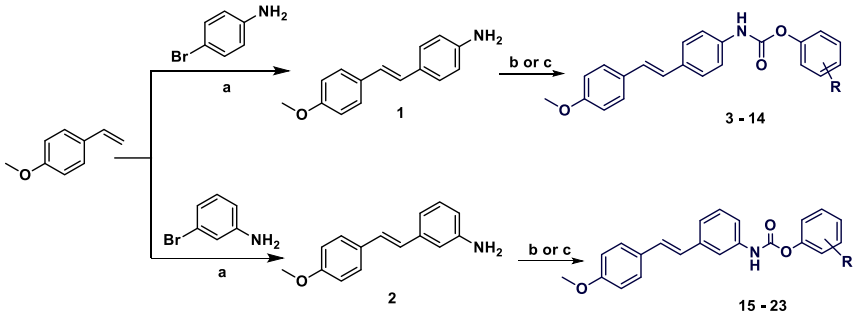

Reagents and conditions: a: $Pd(AcO)_2$, $N(CH_2CH_2OH)_3$, 100°C, 72 h. b: (i) Triphosgene, Et_3N, THF, rt, 10 min; (ii) ArOH, THF, 45°C, 1 h. c: ArOCOCl, pyridine, THF, 0°C 30 min then rt 1 h.

Scheme 1. Synthesis of styryl carbamates **3**–**23**. Reagents and conditions: a: $Pd(AcO)_2$, $N(CH_2CH_2OH)_3$, 100 °C, 72 h. b: (i) Triphosgene, Et_3N, THF, rt, 10 min; (ii) ArOH, THF, 45 °C, 1 h. c: ArOCOCl, pyridine, THF, 0 °C 30 min then rt 1 h.

Table 1
IC_{50} values (μM) for BMS-8 and derivatives **3**–**23**.

Compound	HEK-293	A-549	HT-29	MCF-7
3	>100	17±5	23±10	4±1
4	>100	18±9	32±2	4±2
5	>100	4±2	8±1	1.5±0.2
6	>100	0.34±0.04	5±2	0.3±0.2
7	>100	0.6±0.5	34±4	11±1
8	>100	0.31±0,25	25±2	14±6
9	>100	0.22±0.10	1.3±0.2	0.20±0.17
10	>100	5±2	20±4	9±3
11	>100	0.27±0.16	3±1	0.24±0.12
12	>100	0.24±0.15	1.4±0.3	0.12±0.07
13	>100	0.14±0.08	0.68±0.34	0.24±0.14
14	>100	0.28±0.11	0.60±0.19	0.36±0.24
15	>100	38±1	87±12	27±8
16	>100	96±4	>100	26±10
17	>100	34±2	>100	12±5
18	>100	0.76±0.06	8±1	25±6
19	>100	1.1±0.7	19±3	25±4
20	>100	12±4	24±6	0.29±0.07
21	>100	0.15±0.05	9±4	6±4
22	>100	2.51±1.60	39±7	25±11
23	>100	0.10±0.08	>100	1.2±1
BMS-8	60±10	6±1	19±2	20±3

IC_{50} values are expressed as the compound concentration that inhibits the cell growth by 50 %. Data are the average (±SD) of three experiments.

2.2.2. *Effect on cell viability in A549 monoculture and co-cultures with Jurkat T cells*

To establish the immunomodulatory activity of the selected compounds, first, we studied the effect on tumor cell proliferation in the presence of Jurkat T cells. This assay was carried out using interferon γ stimulated A-549 as the cancer cell line and an excess of immune T cells, 1 to 5 respectively. Assays were performed for 24 h of treatment, using the same doses shown in Table 2 for the selected compounds and BMS-8 as the reference compound. We considered non-treated cells as a control.

We used flow cytometry for the selection of both cell populations and the establishment of living cells for each one. Fig. 5 shows the percentage of living cells related to non-treated ones that is related to control. Interferon γ stimulated cancer cells were treated for 24 h with the compounds at 0.5 μM, except for compound **10** whose dose was 5 μM, in the presence of Jurkat T cells. Then, the different populations of viable cells were detected by using flow cytometry.

The results showed that the tested compounds have a significant immunomodulatory effect. The most outstanding results were found with *p*-chlorophenyl carbamate (**14**) that, when tested at 0.5 μM in monocultures of INF-γ stimulated A-549 cells, did not affect cell viability, while the percentage of living cells related to non-treated ones in the cocultures with Jurkat T cells was reduced to around 40 %. Similar effect was found with *o*-chlorophenyl carbamate (**12**). Moreover, the effect on Jurkat T cell viability is mild with no significant reduction except for compounds *o*-fluoro and *p*-chloro-phenyl carbamates.

2.2.3. *Effect on cancer cell viability in co-cultures with monocytes THP-1*

To establish the immunomodulatory activity of the selected compounds, we studied the effect on INF-γ stimulated tumor cell

Table 2
Working doses of the selected compounds in further biological studies.

Comp.	BMS-8	BMS-8	(9) o-F	(10) m-F	(11) p-F	(12) 0-Cl	(13) m-Cl	(14) p-Cl
Dose	20 μM	100 μM	5 μM	0.5 μM	0.5 μM	0.5 μM	0.5 μM	0.5 μM

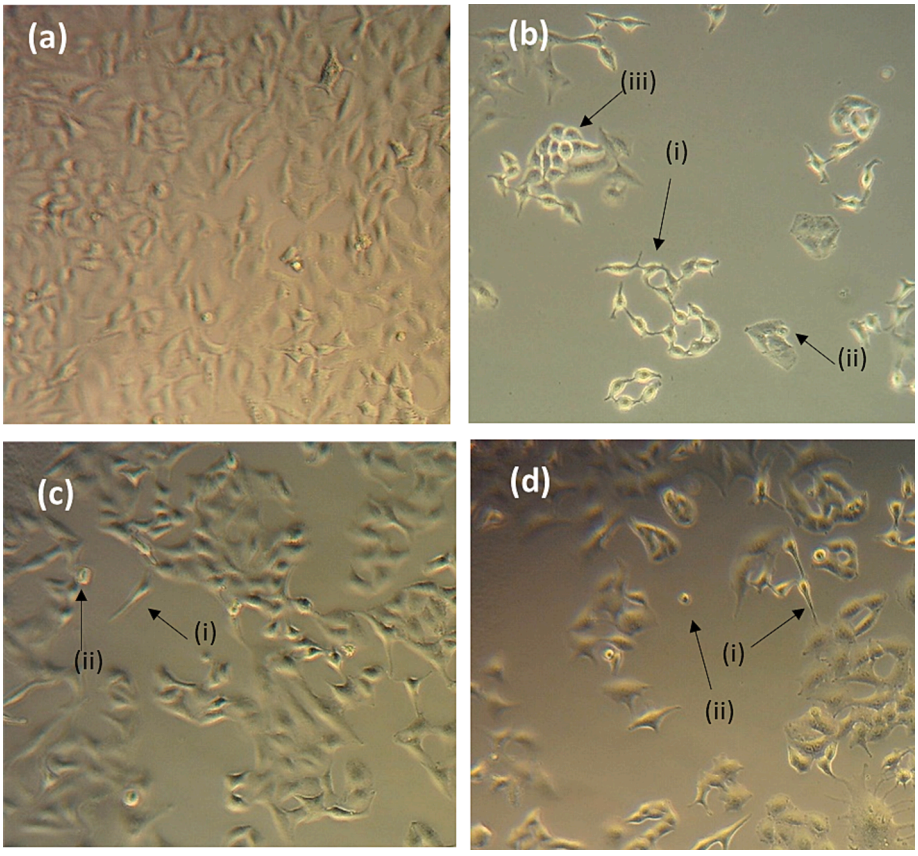

Fig. 4. Morphology of A-549 cells after 48 h of incubation with the corresponding carbamates (a) Control (DMSO-treated cells), (b) *m*-Fluorophenylcarbamate **10** at 5 μM; (c) *p*-Fluorophenylcarbamate **11** at 0.5 μM; (d) *m*-Chlorophenylcarbamate **13** at 0.5 μM.

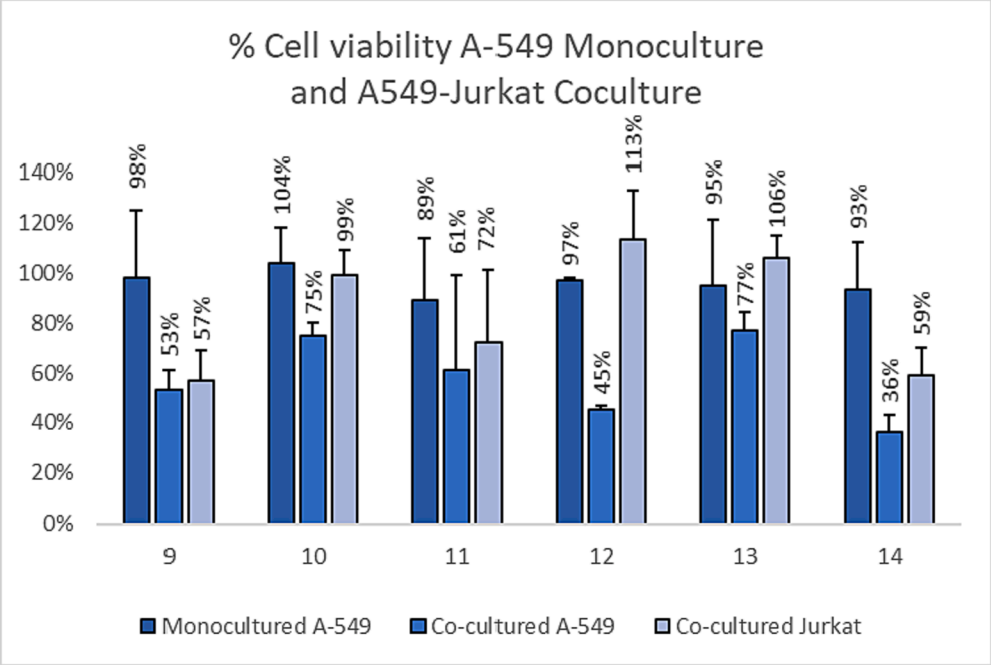

Fig. 5. Relative amount of living cells after treatment with the selected compounds.

proliferation in the presence of human monocytic leukemia cell line THP-1. This assay was carried out using A-549 as the cancer cell line and an excess of monocytes, 1 to 5 respectively. Assays were performed after 24 and 48 h of treatment, using the adequate doses of the selected compounds and BMS-8 as the reference compound.

The results in Fig. 6(a) show that the effect on cancer cell viability was higher after 24 h than after 48 h. All the tested compounds were active causing a reduction above 50 % of viable cancer cells in the presence of monocytes, while in the absence of immune cells compounds exhibited no effect on the living cells related to non-treated cells. In this assay, we included compounds **21** and **23**, bearing the urea unit in *meta*-relative position in the stilbene scaffold, in order to compare the immunomodulatory activity in relation to their structure. Fig. 6(b) showed that in this case the effect is very mild compared to the rest of studied derivatives with a reduction of cancer viable cells around 15 % after 48 h of treatment. Again, the compounds exerted no effect on immune cells when co-cultured with A-549.

2.2.4. Effect on PD-L1 surface cell expression in A-549 monocultured and co-cultured with immune cells

Next step was to determine the effect exerted by the selected compounds on surface PD-L1 expression of cancer cells in similar conditions to the ones in tumor microenvironment. For this, we use the same conditions for the co-cultures described in the previous paragraphs.

That is briefly, interferon-γ stimulated A-549 cells were treated for 24 h with the compounds in the presence of Jurkat T cells or in the presence of THP-1. Then, cells were fixed and treated with anti-PD-L1 conjugated to AlexaFluor®647. We used flow cytometry for the selection of both cell populations and the establishment of living cells for each one where proportion of PD-L1 expression was measured related to non-treated cells.

Fig. 7 shows the percentage of PD-L1 in the different cell populations related to control at 24 h.

Results showed that chlorophenyl carbamates were the most active as they were able to inhibit about 30 % of PD-L1 surface on cancer cells. On the other hand, when compared with monocytes, fluoroderivatives exhibited a milder effect when cancer cells were co-cultured with T cells.

2.2.5. Study of the blocking effect on the binding of the PD-1/PD-L1 binding

After having established the immunomodulatory action of the derivatives on A-549 co-cultures with immune cells, we study their effect on PD-1/PD-L1 binding by competitive ELISA assay [30]. This assay is based on the high affinity between PD-1 and PD-L1 and it was carried out at 20 μM concentration in DMSO for all derivatives.

The results, depicted in Fig. 8, show that BMS-8, which is our reference compound, is the most active one with inhibition rates around 80 %, while compounds **9** (*o*-F), **11** (*p*-F) and **14** (*p*-Cl) are the most active blocking about 30 % the binding between both proteins.

2.2.6. Effect on monocytes surface cell expression of CD80, CD11b and PD-L1 when co-cultured with A-549

Cancer and its associated therapies have been shown to induce functional changes in monocytes, including acquiring immunosuppressive activity in the tumor microenvironment, which is associated with the expression of CD11b. This cluster of differentiation is an integrin that, when it binds to CD18, accelerates the invasiveness and metastasis of cancer cells and promotes systemic inflammation of the TME [33]. Reducing the expression of CD11b has been identified as a promising target for immunomodulation in anti-cancer therapies [34]. Therefore, we decided to investigate the effect of our compounds on CD11b in THP-1 cells co-cultured with A-549 together with CD80, a common marker for these cells, and also on PD-L1 that can be present in the pro-inflammatory monocytes cell surface [35].

For this, we use the same conditions for the co-cultures described in the previous sections. In this case, the study was performed on the collected cell culture from each well and gating living THP-1 cell population. Fig. 9 shows the results obtained when we determined the percentage of CD80, CD11b and PD-L1 expression in membrane THP-1, related to non-treated cells, when they were co-cultured with A-549 and with our compounds.

It can be observed that neither of the compounds have any effect on CD80 expressions but our derivatives were able to reduce the presence of CD11b pro-inflammatory marker in the monocyte cell surface. Compounds **10** (*p*-F), **9** (*o*-F) and **12** (*o*-Cl) were the most active ones with inhibition rates above 70 %. Besides, all the compounds had a mild effect

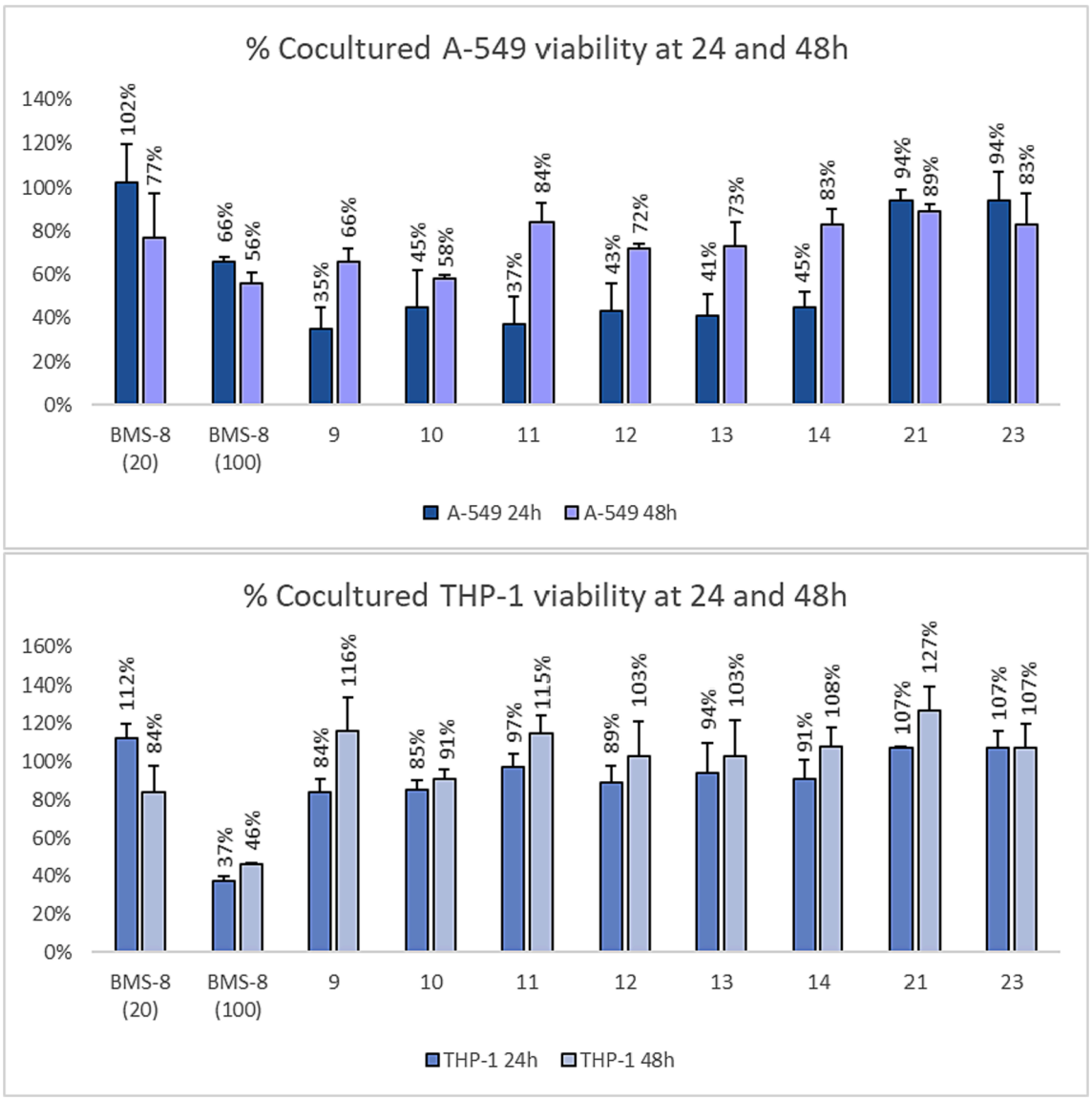

Fig. 6. Relative amount of living cells after treatment with the selected compounds in co-cultures of A-549 and THP-1 at 24 and 48 h. (a) A-549 living cells; (b) THP-1 living cells.

on the expression of PD-L1, outstanding **10**, **12** and **13** with around 65 % of expression.

2.2.7. Study of the effect on the secretion of pro-inflammatory cytokines TNF-α, IL-6 and SAA-1

We selected some of three representative compounds according to the results obtained along all the previous studies to determine their effect on the secretion of IL-6, SAA-1 and TNF-α into the cell medium. Compounds selected were carbamates **10** (*m*-F), **11** (*p*-F) and **13** (*m*-Cl). We measured the level of the secreted cytokines into the cell medium from monocultures of A-549, monocultures of THP-1 and, also, from co-cultures of A-549 and THP-1 after 24 h of treatment with the selected compounds at doses of 5 μM for **10** and 0.5 μM for **11** and **13**. Measurements were carried out by ELISA assay (see Fig. 10).

As regards TNF-α, it was only detected on sample media from monocultured THP-1 and, as it can be seen in Fig. 10, none of the compounds hardly affected the levels of secretion when compared to non-treated cells.

In line with the results obtained for the THP-1 monoculture samples, we observed that compounds **10** and **13** did not affect the level of IL-6 secretion by monocytes, whereas compound **11** slightly stimulated secretion. This slight stimulation of IL-6 secretion was also observed in monocultures of cancer cells, but in co-cultures compounds **10** and **13** were able to reduce the secretion of the cytokine by 30 %.

On the other hand, as for SAA-1, compounds did not affect the level of secretion of this protein in monocyte monocultures, showing a very weak inhibitory effect on secretion in cancer cell monocultures, while again the maximum inhibitory effect was observed in co-cultures of A-549 and THP-1. In these cases, all three compounds achieved a reduction of approximately 35 % of SAA-1 in the co-culture medium.

3. Conclusion

In this study we have synthesized a set of compounds bearing a *p*-methoxystyryl and an aryl carbamate motif in both 1,3 and 1,4 relative positions and we have identified 1,4-[*p*-(methoxystyryl)] fluor and chlorophneylcarbamates **9**–**14** as potential oncoimmunomodulary drug candidates. When screening for in vitro activity, these derivatives significantly inhibited A-549 and MCF-7 cell proliferation at high nanomolar concentrations and, moreover, they reduced till 60 % the number of A-549 living cells when co-cultured in the presence of Jurkat T-cells or monocytes THP-1, with no effect on immune cell

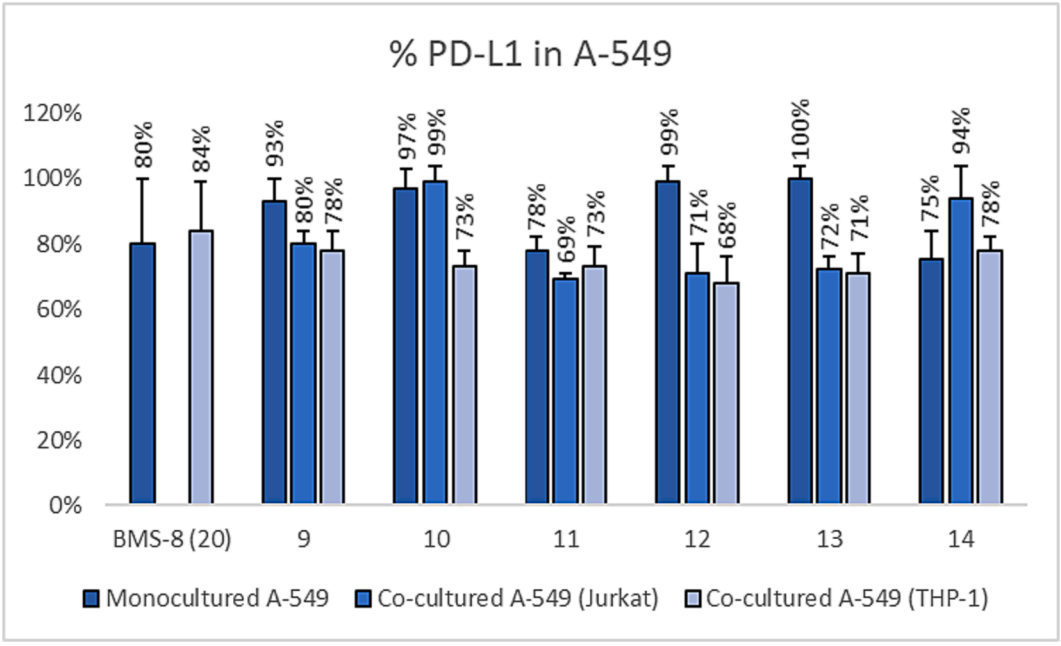

Fig. 7. Relative amount of PD-L1 in A-549.

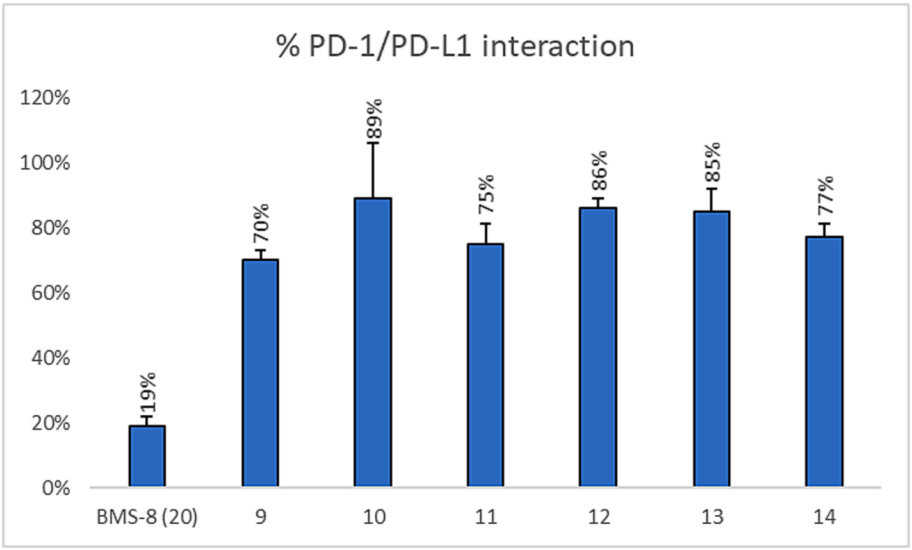

Fig. 8. PD-1/PD-L1 binding activity related to control (DMSO).

proliferations. In addition, we have also shown that compounds **9**–**14** exhibited good anti-inflammatory profiles with secretion levels of the inflammatory factors TNF-α, IL-6 and SAA-1 around 70 % compared to non-treated cells. In terms of mechanism of action, these compounds can effectively downregulate the expression of PD-L1 in cancer and the expression of both PD-L1 and CD-11b monocytes altogether with a blockage of the PD-1/PD-L1 binding interaction.

This may be an important molecular mechanism by which these compounds reduce dramatically the immunosuppressive atmosphere in the TME.

4. Experimental section

4.1. Chemistry

4.1.1. General procedures

^{1}H and ^{13}C NMR spectra were measured at 25 °C. The signals of the deuterated solvent ($CDCl_3$ and DMSO-d_6) were taken as the reference. Multiplicity assignments of ^{13}C signals were made by means of the DEPT pulse sequence. Complete signal assignments in ^{1}H and ^{13}C NMR spectra were made with the aid of 2D homo- and heteronuclear pulse sequences (COSY, HSQC, HMBC). Infrared spectra were recorded using KBr plates. High resolution mass spectra were recorded using electrospray ionization–mass spectrometry (ESI–MS). Experiments which required an inert atmosphere were carried out under dry N_2 in oven-dried glassware. Commercially available reagents were used as received.

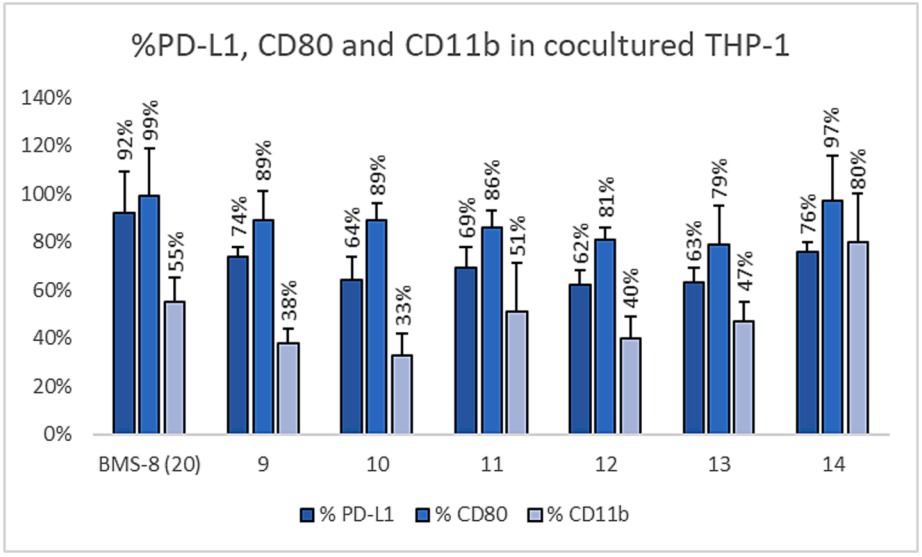

Fig. 9. Relative amount of PD-L1, CD80 and CD11b in THP-1.

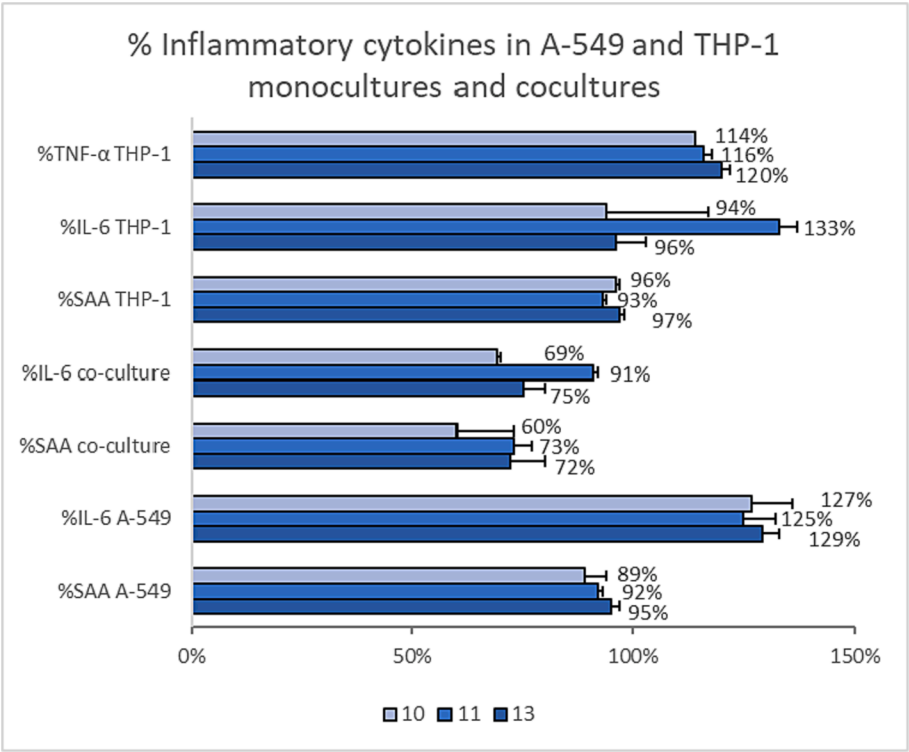

Fig. 10. Relative amount of secreted cytokines IL-6 TNF-α and SAA-1 into the cell medium.

4.1.2. Experimental procedure for synthesis of styryls by method a

A solution of the corresponding bromoaniline (1 eq.), 4-methoxy styrene (1 eq.) and $Pd(AcO)_2$ (0.01 eq.) in triethanolamine (1.2 mL/mmol) was stirred, under N_2, at 100 °C for 72 h. After cooling at room temperature, the reaction mixture was extracted with AcOEt (3×15 mL) and the combined organic layers were washed with brine, dried on anhydrous $MgSO_4$ and concentrated under reduced pressure. The residue was purified by column chromatography on silica gel using mixtures of Hexanes-EtOAc as eluent (7:3→1:1).

4.1.3. Experimental procedure for the synthesis of carbamates by method b

A solution of the stilbene (1 eq.) in THF (4 mL/mmol) was added to a solution of triphosgene (2.1 eq.) in THF (0.7 mL/mmol). The resulting mixture was stirred in the dark for 10 min at rt. Then Et_3N (30,7 eq.) was slowly added and the resulting residue was resuspended in THF (5.7 eq.). The corresponding phenol (5.7 eq.) was added to the mixture which was stirred in the dark for 1 h at 45 °C. After this time, volatiles were removed under reduced pressure and the remaining residue was dissolved in acetone. The precipitated was discarded by simple filtration and the filtrate was concentrated under reduced pressure. The residue was purified by column chromatography on silica-gel using mixtures of Hexanes-EtOAc as eluent (9:1→1:1).

4.1.4. Experimental procedure for synthesis of carbamates by method c

A solution of the stilbene (1 eq.) in THF (5 mL/mmol) was cooled at 0 °C and anhydrous pyridine (2.4 eq.) and the corresponding phenyl chloroformate (1.4 eq.) were added under N_2 atmosphere. The resulting mixture was stirred in the dark for 20 min at 0 °C and then for 1 h at rt. After this time, H_2O (5 mL/mmol) and HCl 1 M (2.5 mL/mmol) were added to the reaction mixture, which was then extracted with CH_2Cl_2 (3×20 mL). The organic layer was washed with brine and then dried on anhydrous Na_2SO_4. Removal of volatiles under reduced pressure afforded a residue which was purified by column chromatography on silica-gel using mixtures of Hexanes-EtOAc as eluent (9:1→1:1).

4.2. Biological studies

4.2.1. Cell culture

Cell culture media were purchased from Gibco (Grand Island, NY). Fetal bovine serum (FBS) was obtained from Harlan-Seralab (Belton, U. K.). Supplements and other chemicals not listed in this section were obtained from Sigma Chemical Co. (St. Louis, MO). Plastics for cell culture were supplied by Thermo Scientific BioLite. All tested compounds were dissolved in DMSO at a concentration of 20 mM and stored at −20 °C until use.

HT-29, A-549, MCF-7 and HEK-293 cell lines were maintained in Dulbecco's modified Eagle's medium (DMEM) containing glucose (1 g/L), glutamine (2 mM), penicillin (50 μg/mL), streptomycin (50 μg/mL), and amphotericin B (1.25 μg/mL), supplemented with 10 % FBS. For the HMEC-1 cell line, it was used Dulbecco's modified Eagle medium (DMEM)/Low glucose containing glutamine (2 mM), penicillin (50 μg/mL), streptomycin (50 μg/mL, and amphotericin B (1.25 μg/mL) supplemented with 10 % FBS. For the development of the antiangiogenesis test, the HMEC-1 cells were seeded on matrigel in EGM-2MV Medium supplemented with EGM-2MV SingleQuots (Lonza, CA, USA).

4.2.2. Cell proliferation assay

5×10^3 cells per well were incubated in 96-well plates with serial dilutions of the tested compounds in a total volume of 100 μL of their growth media. 3-(4,5-dimethylthiazol-2-yl)-2,5-diphenyltetrazolium bromide (MTT; Sigma Chemical Co.) dye reduction assay in 96-well microplates was used. 10 μL of MTT (5 mg/mL in phosphate-buffered saline, PBS) was added to each well after 2 days of incubation (37 °C, 5 % CO_2 in a humid atmosphere). The plate was incubated for a further 3 h (37 °C). After that, the supernatant was discarded and 100 μL of DMSO were added in order to dissolve formazan crystals. The absorbance was read at 550 nm by spectro-photometry. For all concentrations of compound, cell viability was expressed as the percentage of the ratio between the mean absorbance of treated cells and the mean absorbance of untreated cells. Three independent experiments were performed, and the IC_{50} values (i.e., concentration half inhibiting cell proliferation) were graphically determined using GraphPad Prism 4 software.

4.2.3. PD-L1, CD80 and CD-11b relative quantification by flow cytometry

To study the effect of the compounds on every biological target in cancer cell lines compounds were used at the doses shown in Table 2. For the assay, 10^5 cells per well were incubated for 24 h with the corresponding dose of the tested compound in a total volume of 500 μL of their growth media. To detect membrane PD-L1, CD80 or CD-11b, after cell treatments, they were collected, fixed with 4 % in PBS paraformaldehyde and stained with FITC Mouse monoclonal Anti-Human CD80 (ab18279), Alexa Fluor® 647 Rabbit monoclonal Anti-CD11b (ab307523) and Alexa Fluor® 647 Rabbit monoclonal Anti-PD-L1 (ab215251).

4.2.4. Cell viability evaluation in co-cultures

To study the effect of the compounds on cancer cell viability in co-culture with Jurkat T or with THP-1 cells, 10^5 of A-549 cells line per well were seeded and incubated for 24 h. Then, medium was changed by a cell culture medium supplemented with IFN-γ (10 ng/ml; human, Invitrogen®) containing 5×10^5 of Jurkat T or THP-1 cells per well and the corresponding compound at adequated dose in μM. For the positive control DMSO was added. After 24 or 48 h of incubation, supernatants were collected to determine immune living cells. Besides, stained cancer cells were collected with trypsin. Both types of suspension cells were fixed with 4 % in PBS paraformaldehyde and counted by flow cytometry.

4.2.5. Secretion of cytokines quantification by ELISA assay

To study the effect of the compounds on secreted cytokines, 10^5 cells per well were incubated for 24 h with the corresponding dose of the tested compound in a total volume of 500 μL of their growth media. These media were collected from monocultures or from co-cultures and used as a sample in the Invitrogen® Human IL-6 ELISA Kit (cat: KHC0061), Invitrogen® Human TNF-α ELISA Kit (cat: KHC3014) Human SAA-1 ELISA Kit (ab100635).

4.2.6. Statistical analysis

Statistical significance was evaluated using one-way ANOVA. Data were expressed as means ± SD for triplicates. The level of statistical significance differences was set as P values of $p < 0.05$.

CRediT authorship contribution statement

Amelia Bou-Puerto: Writing – review & editing, Writing – original draft, Visualization, Validation, Software, Methodology, Investigation, Formal analysis. **Miguel Carda:** Writing – review & editing, Visualization, Validation, Supervision, Resources, Methodology, Funding acquisition, Data curation, Conceptualization. **Eva Falomir:** Writing – review & editing, Writing – original draft, Supervision, Software, Resources, Project administration, Methodology, Investigation, Funding acquisition, Formal analysis, Data curation.

Declaration of competing interest

The authors declare the following financial interests/personal relationships which may be considered as potential competing interests: Eva Falomir reports financial support was provided by Ministry of Economy and Competitiveness. Eva Falomir reports financial support was provided by ministry of science and innovation. Eva Falomir reports financial support was provided by ERDF A way of making Europe. Amelia Bou-Puerto reports financial support was provided by European Union. Amelia Bou-Puerto reports financial support was provided by Ministry of Labour Employment and Social Economy. If there are other authors, they declare that they have no known competing financial interests or personal relationships that could have appeared to influence the work reported in this paper.

Acknowledgments

Authors are grateful to SCIC of the Universitat Jaume I for providing NMR, mass spectrometry and flow cytometry facilities.

Funding

This work was supported by the Grant PID2021-126277OB-100 funded by MCIN/AEI/https://doi.org/10.13039/501100011033 and by "ERDF A way of making Europe"; by Ministry of Economy and Competitiveness (project RTI2018-097345-B-I00) and by Universitat Jaume I (project UJI-B2021-46). A.B-P. thanks to European Union– Next Generation EU, Public Service of State Employment-SEPE and Ministry of Labour and Social Economy for its contract 20881- Programa Investigo, within the Recovery, Transformation and Resilience Plan.

References

[1] T.L. Whiteside, The tumor microenvironment and its role in promoting tumor growth, Oncogene. 27 (2008) 5904–5912, https://doi.org/10.1038/onc.2008.271.

[2] R. Baghban, L. Roshangar, R. Jahanban-Esfahlan, Tumor microenvironment complexity and therapeutic implications at a glance, Cell Commun. Signal. 18 (2020) 59–70, https://doi.org/10.1186/s12964-020-0530-4.

[3] N. El-Sayes, A. Vito, K. Mossman, Tumor heterogeneity: a great barrier in the age of cancer immunotherapy, Cancers 13(4) (2021) 806, https://doi.org/10.3390/cancers13040806.

[4] C. Roma-Rodrigues, R. Mendes, P.V. Baptista, A.R. Fernandes, Targeting Tumor Microenvironment for Cancer Therapy, Int. J. Mol. Sci. 20 (2019) 840, https://doi.org/10.3390/ijms20040840.

[5] M.-Z. Jin, W.-L. Jin, The updated landscape of tumor microenvironment and drug repurposing, Signal Transduct. and Targeted Ther. 5 (2020) 166, https://doi.org/10.1038/s41392-020-00280-x.

[6] L. Bejarano, M.J.C. Jordão, J. Joyce, Therapeutic Targeting of the Tumor Microenvironment, Cancer Discov. 11 (2021) 933–959, https://doi.org/10.1158/2159-8290.CD-20-1808.

[7] K. Dzobo, D.A. Senthebane, C. Dandara, The Tumor Microenvironment in Tumorigenesis and Therapy Resistance Revisited, Cancers 15 (2023) 376, https://doi.org/10.3390/cancers15020376.

[8] A. Tiwari, R. Trivedi, S.Y. Lin, Tumor microenvironment: barrier or opportunity towards effective cancer therapy, J Biomed Sci 29 (2022) 83–110, https://doi.org/10.1186/s12929-022-00866-3.

[9] L.V. Marchenko, A.D. Nikotina, N.D. Aksenov, J.V. Smagina, B.A. Margulis, I. V. Guzhova, Phenotypic Characteristics of Macrophages and Tumor Cells in Coculture, Cell and Tissue Biol. 60 (2018) 357–364, https://doi.org/10.1134/S1990519X18050036.

[10] K. Mittal, J. Ebos, B. Rini, Angiogenesis and the tumor microenvironment: vascular endothelial growth factor and beyond, Rev. Semin Oncol. 41 (2014) 235–251.

[11] F.R. Greten, S.I. Grivennikov, Inflammation and Cancer: Triggers, Mechanisms, and Consequences, Immunity 41 (2019) 27–35.

[12] M. Nagano, K. Saito, Y. Kozuka, T. Mizuno, T. Ogawa, M. Katayama, PD-L1 expression on circulating monocytes in patients with breast cancer. Breast Cancer, locally advanced, Ann. Oncol. 9 (2018) 10–21, https://doi.org/10.1093/annonc/mdy427.008.

[13] Alexander, W. The Checkpoint Immunotherapy Revolution: What Started as a Trickle Has Become a Flood, Despite Some Daunting Adverse Effects; New Drugs, Indications, and Combinations Continue to Emerge. P T. 2016, 41, 185-91. PMID: 26957887; PMCID: PMC4771089.

[14] Y. Zhang, Z. Zhang, The history and advances in cancer immunotherapy: understanding the characteristics of tumor-infiltrating immune cells and their therapeutic implications, Cell. Mol. Immunol. 17 (2020) 807–821.

[15] J. Chen, Y. Wei, W. Yang, Q. Huang, Y. Chen, K. Zeng, J. Chen, IL6: The Link Between Inflammation, Immunity and Breast Cancer. Front, Oncol. 12 (2022) 903800, https://doi.org/10.3389/fonc.2022.903800.

[16] D.T. Fisher, M.M. Appenheimer, S.S. Evans, The Two Faces of IL-6 in the Tumor Microenvironment, Semin. Immunol. 26 (2014) 38–47, https://doi.org/10.1016/j.smim.2014.01.008.

[17] J. Mauer, J.L. Denson, C. Bruning, Versatile functions for IL-6 in metabolism and cancer, Trends in Immunol. 36 (2015) 92–101, https://doi.org/10.1016/j.it.2014.12.008.

[18] G.H. Sack, Serum amyloid A – a review, Molecular Medicine 24 (2018) 1–27, https://doi.org/10.1186/s10020-018-0047-0.

[19] S.A. Moshkovskii, Why do cancer cells produce serum amyloid A acute-phase protein? Biochemistry 77 (2012) 339–341, https://doi.org/10.1134/S0006297912040037.

[20] R.J. Flores, A. Kelly, Y. Li, X. Chen, C. McGee, M. Krailo, D.A. Barkauskas, J. Hicks, T.-K. Mana, The Prognostic Significance of Circulating Serum Amyloid A and CXC Chemokine Ligand 4 in Osteosarcoma, Pediatr Blood Cancer. 64 (2017) 1–14, https://doi.org/10.1002/pbc.26659.

[21] S.A. Kinkley, L.G. William, G.S. Bagshaw, S-P. Tam, R. Kisilevsky, The path of murine serum amyloid A through peritoneal macrophages, Amyloid 13 (2006) 123–134, https://doi.org/10.1080/13506120600877201.

[22] O. Trott, A.J. Olson, Autodock Vina: improving the speed and accuracy of docking with a new scoring function, efficient optimization and multithreading, J. Comput. Chem. 31 (2010) 455–461, https://doi.org/10.1002/jcc.21334.].

[23] M. McTigue, B.W. Murray, J.H. Chen, Y.L. Deng, J. Solowiej, R.S. Kania, Molecular conformations, interactions, and properties associated with drug efficiency and clinical performance among VEGFR TK inhibitors, Proc Natl Acad Sci USA 109 (2012) 18281–18289, https://doi.org/10.1073/pnas.120775910915.

[24] K.M. Zak, P. Grudnik, K. Guzik, B.J. Zieba, B. Musielak, A. Dömling, G. Dubin, T. A. Holak, Structural basis for small molecule targeting of the programmed death ligand 1 (PD-L1), Oncotarget. 7 (2016) 30323–30335, https://doi.org/10.18632/oncotarget.8730.

[25] L. Conesa-Milián, E. Falomir, J. Murga, M. Carda, J.A. Marco, Synthesis and biological evaluation as antiangiogenic agents of ureas derived from 3′-aminocombretastatin A-4, Eur. J. Med. Chem. 162 (2019) 781–792, https://doi.org/10.1016/j.ejmech.2018.11.023.

[26] C. Martín-Beltrán, R. Gil-Edo, G. Hernández-Ribelles, R. Agut, P. Marí-Mezquita, M. Carda, E. Falomir, Aryl Urea Based Scaffolds for Multitarget Drug Discovery in Anticancer Immunotherapies, Pharmaceuticals 14 (2021) 337, https://doi.org/10.3390/ph14040337.

[27] A. Pla-López, R. Castillo, R. Cejudo-Marín, O. García-Pedrero, M. Bakir-Laso, E. Falomir, M. Carda, Synthesis and Bio-logical Evaluation of Small Molecules as Potential Anticancer Multitarget Agents, Int. J. Mol. Sci. 23 (2022) 7049–7064, https://doi.org/10.3390/ijms23137049.

[28] R. Gil-Edo, S. Espejo, E. Falomir, M. Carda, Synthesis and Biological Evaluation of Potential Oncoimmunomodulator Agents, Int. J. Mol. Sci. 24 (2023) 2614, https://doi.org/10.3390/ijms24032614.

[29] A. Montfort, C. Colacios, T. Levade, N. Andriu-Abadie, N. Meyer, S. Ségui, The TNF paradox in cancer Progression and Immunotherapy, Front. Immunol. 10 (2019) 1818–1823, https://doi.org/10.3389/firmmu.2019.01818.

[30] H. Ji Li, L. Wang, Triethanolamine as an Efficient and Reusable Base, Ligand and Reaction Medium for Phosphane-Free Palladium-Catalyzed Heck Reactions, Eur. J. Org. Chem. (2006) 5099–5102.

[31] L. Yang, G. Li, S. Ma, C. Zou, S. Zhou, Q. Sun, C. Cheng, X. Chen, L. Wang, S. Feng, L. Li, S. Yang, Structure-activity relationship studies of pyrazolo[3,4-d] pyrimidine derivatives leading to the discovery of a novel multikinase inhibitor that potently inhibits FLT3 and VEGFR2 and evaluation of its activity against acute myeloid leukemia in vitro and in vivo, J. Med. Chem. 56 (2013) 1641–1655.

[32] L. Zhang, W. Xia, B. Wang, Y. Luo, W. Lu, Convenient synthesis of sorafenib and its derivatives, Synth. Commun. 41 (2011) 3140–3146.

[33] C. Pfluecke, S. Wydra, K. Berndt, D. Tarnowski, M. Cybularz, P. Barthel, A. Linke, K. Ibrahim, D.M. Poitz, CD11b expression on monocytes and data of inflammatory parameters in dependence of early mortality, Data Brief. 31 (2020) 105798, https://doi.org/10.1016/j.dib.2020.105798.

[34] L.E. Padgett, D.J. Araujo, C.C. Hedrick, C.E. Olingy, Functional crosstalk between T cells and monocytes in cancer and atherosclerosis, J. Leukoc. Biol. 108 (2020) 297–308, https://doi.org/10.1002/JLB.1MIR0420-076R.

[35] W. Zhang, Y. Liu, Z. Yan, IL-6 promotes PD-L1 expression in monocytes and macrophages by decreasing protein tyrosine phosphatase receptor type O expression in human hepatocellular carcinoma, J. Immunother. Cancer 8 (2020) e000285.